Determination of subcritical crack growth on glass in water from lifetime measurements on Knoop-cracked specimens

T. FETT, D. MUNZ*
*Institut für Material- und Festkörperforschung IV, Kernforschungszentrum Karlsruhe, Karlsruhe, W. Germany and *Institut für Zuverlässigkeit und Schadenskunde im Maschinenbau, Universität Karlsruhe, Karlsruhe, W. Germany*

K. KELLER
Institut für Keramik im Maschinenbau, Universität Karlsruhe, Karlsruhe, W. Germany

The crack growth behaviour of glass in water is investigated by use of lifetime measurements carried out with Knoop-damaged specimens in four-point bending tests. The method is outlined in detail and the crack growth law – exhibiting a threshold stress intensity factor $K_{th} = 0.35\,\mathrm{MPa\,m^{1/2}}$ – is determined. The initial and final crack size data as well as the fracture toughness are given by Weibull representations.

1. Introduction

The effect of subcritical crack growth appears in most ceramic materials. In case of linear-elastic material behaviour the crack growth rates are dependent only on the stress intensity factor K_I which is defined by

$$K_I = \sigma a^{1/2} Y \quad (1)$$

where a is the crack depth, σ the applied stress and Y a geometric function, which depends on the crack shape and the specimen geometry. The knowledge of the relation

$$da/dt = v(K_I) \quad (2)$$

is of high importance for lifetime calculations. Whilst the dependency can often be described by a simple power-law for moderate crack-growth rates over several decades, a deviation at very low crack growth rates has to be taken into consideration.

Especially for glass in water, a threshold of subcritical crack growth most likely exists. Already more than 10 years ago the measurements of Wiederhorn and Bolz [1] and Evans [2] using the "double cantilever beam technique" (DCB) and the "double torsion method" (DTM), respectively, showed a typical threshold behaviour for macroscopic cracks. Due to the study of Fournier and Naudin [3] on the reliability of the DTM for extremely low crack growth rates the DTM results became unsafe, because only crack growth rates $v > 10^{-9}\,\mathrm{m\,sec^{-1}}$ seem to be sufficiently accurate.

Various theoretical investigations of subcritical crack extension – mostly based on the idea that thermal transients both break and re-establish bonds – predict the existence of a threshold as well [4–7].

As a simple method to determine extremely low crack growth rates, the lifetime measurement seems to be most appropriate.

2. Basic formulae

The lifetime t_f of a specimen loaded with an initial stress intensity factor K_{Ii} can be written

$$t_f = \frac{2}{(\sigma Y_i)^2} \int_{K_{Ii}}^{K_{Ic}} \left(\frac{1}{v}\right) K_I \, dK_I \quad (3)$$

where Y_i is the geometric function of the initial crack, and K_{Ic} is the fracture toughness of the material considered. If the initial stress intensity factor is not constant along the crack tip line, the maximum occurring value has to be inserted.

To evaluate lifetime measurements with different stresses it is suitable to consider the quantity

$$t_f \sigma^2 Y_i^2 = 2 \int_{K_{Ii}}^{K_{Ic}} \left(\frac{1}{v}\right) K_I \, dK_I \quad (4)$$

which is only a function of the initial stress intensity factor.

By measuring the lifetime t_f for different adjusted initial stress intensity factors K_{Ii} it is possible to determine $v(K_{Ii})$ from Equation 4. An appropriate procedure for the evaluation of crack growth rates from lifetime measurements in static bending tests has been proposed [8]. This method does not require any knowledge of the v–K_I dependency.

In the work of Fett and Munz [8] a constant load was applied for a test series and the variation of K_{Ii} values was caused by scatter in crack sizes of the natural small cracks. Since it was not possible to measure the initial crack sizes directly, their distribution had to be concluded from measurements of the so-called "inert bending strength".

Another possibility for varying the initial stress intensity factor K_{Ii} is the application of various bending stresses using approximately uniform cracks. Such small and sharp cracks can be produced in Knoop indentation tests.

0022–2461/88 $03.00 + .12 © *1988 Chapman and Hall Ltd.*

By differentiating Equation 4 with respect to the initial stress intensity factor K_{Ii} one obtains [8]

$$v(K_{Ii}) = -\frac{2}{t_f\sigma^2}\left(\frac{K_{Ii}}{Y_i}\right)^2 \frac{\mathrm{d}[\log(K_{Ii})]}{\mathrm{d}[\log(t_f\sigma^2 Y_i^2)]} \quad (5)$$

Under the assumption that the crack growth law may be expressed by a power law

$$v(K_I) = A K_I^n \quad (6)$$

Equation 4 can be integrated and this yields the well-known lifetime formula

$$t_f \simeq \frac{2}{A\sigma^2 Y^2 (N-2)} K_{Ii}^{-(n-2)} \quad (7)$$

but in this study such a strong restriction is not necessary.

3. Procedures for determination of crack growth rates

Two different procedures are possible to evaluate Equation 5:

(i) If the contour of the initial crack after failure can be detected with a microscope, the two half-axes a_i and c_i of the semi-elliptic crack can be measured and Y_i can be calculated. Because a_i is known, Equation 5 can be rewritten as

$$v(K_{Ii}) = -\left(\frac{a_i}{t_f}\right) \frac{\mathrm{d}[\log(K_{Ii}^2)]}{\mathrm{d}[\log(\sigma^2 t_f Y_i^2)]} \quad (8)$$

The initial stress intensity factor has to be known for correlating the crack growth rates by a v–K_I plot. This evaluation is possible for Knoop cracks in glass. Fig. 1 shows such a crack.

(ii) If the cracks cannot be identified after failure, the initial crack size can be replaced by the inert bending strength

$$\sigma_c = \frac{K_{Ic}}{Y_i a_i^{1/2}} \quad (9)$$

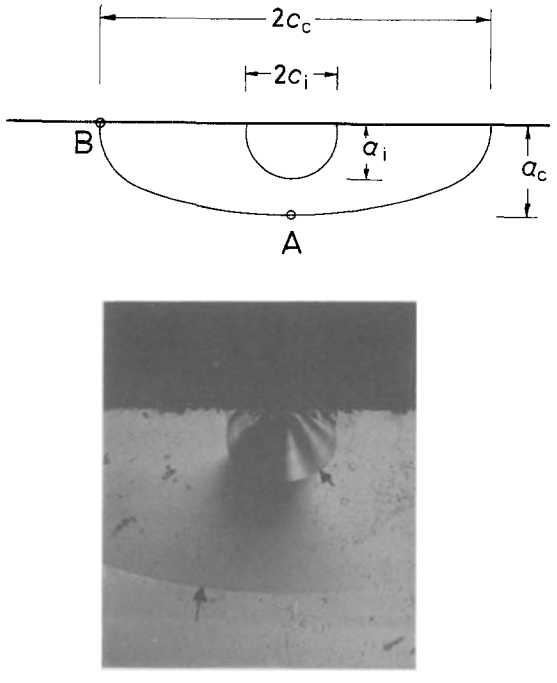

Figure 1 Fracture mirror after failure in a lifetime test. Inner contour: initial crack size after indentation test. Outer contour: crack size at failure.

i.e. the strength without subcritical crack extension. Inserting Equation 9 into Equation 5 gives a modified relation

$$v(K_{Ii}) = -\frac{2}{t_f\sigma_c^2}\left(\frac{K_{Ic}}{Y_i}\right)^2 \frac{\mathrm{d}[\log(K_{Ii}/K_{Ic})]}{\mathrm{d}[\log(t_f\sigma^2 Y_i^2)]} \quad (10)$$

where the initial value of Y_i is assumed to be the same for all cracks produced under identical conditions.

In this study the first method was applied.

4. Experiments and results

4.1. Measurements

The experiments were performed with 4 mm × 5 mm × 45 mm specimen cut out from plates of a commercial borosilicate glass (BK 7, Glaswerke Schott, Mainz) with a transition temperature of 560° C. After machining, the specimens were annealed at 470° C for 5 h. By Knoop indentation with 50 N indentation load the specimens were damaged in a controlled manner.

The specimens were then annealed again (470° C, 5 h) to remove stresses at the crack tip due to wedging forces in the damaged region below the Knoop indentor.

In static four-point bending tests, lifetimes were determined in water at 20° C for several bending stresses. The tests were finished after 1000 h and the survival specimens qualified as "through runs". The results are shown in Fig. 2. It is remarkable that no failure occurs below 18 MPa, although fracture would be expected there by a linear extrapolation of the measured lifetime points. The initial crack sizes a_i and the initial aspect ratios a_i/c_i were measured under an optical microscope.

In Fig. 3 the data for the initial cracks are plotted as Weibull diagrams. By use of the "maximum likelihood method" one obtains for the crack depth a_i a median value (i.e. the value for 50% cumulative frequency) of

$$\langle a_i \rangle = 0.32$$

and a Weibull parameter

$$m(a_i) = 5.5$$

For the crack length c_i one obtains

$$\langle c_i \rangle = 0.275 \qquad m(c_i) = 14$$

and for the initial aspect ratio a_i/c_i

$$\langle a_i/c_i \rangle = 1.2 \qquad m(a_i/c_i) = 7.1$$

Due to Equation 9 the Weibull modulus for the inert bending strength yields $m(\sigma_c) = 2m(a_i) = 11$. This value is higher than one can expect in the case of natural crack distributions.

By plotting the initial aspect ratio a_i/c_i as a function of the initial crack depth a_i (Fig. 4) one can see that there is no independence between the two characteristic crack data.

4.2. Calculation of stress intensity factors

To calculate the initial stress intensity factors the correction function Y as a function of the aspect ratio a/c and the normalized crack depth a/t (t = thickness of

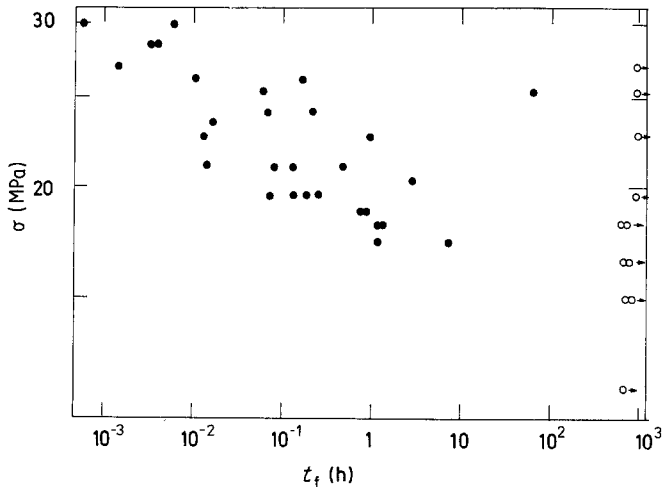

Figure 2 Lifetimes of Knoop-damaged glass specimens as a function of the bending stress applied.

the specimen) has to be known. Extensive computations of correction functions for semi-elliptical surface cracks were performed by Newman and Raju [9] in the ranges $0.2 \leqslant (a/c) \leqslant 2$ and $0 \leqslant (a/t) \leqslant 0.8$ for tension as well as for bending using the finite-element method. Unfortunately, only the bending data for $(a/c) \leqslant 1$ were expressed by formulae, so one has to interpolate their tabulated values to obtain Y for $(a/c) > 1$.

4.2.1. Local stress intensity factors

If Y is only of interest for the *deepest point* of the crack (Y_A) and the *surface points* (Y_B) – which is the case in this investigation – one can fit the data by

$$Y_A = -0.39443 + 2.10145\left(\frac{a}{c}\right)^{-2/3} - 0.544673\left(\frac{a}{c}\right)^{-4/3} - \left[1.9774 - 0.4207\left(\frac{a}{c}\right)\right]\left(\frac{a}{t}\right) \quad (11)$$

$$Y_B = 1.28\left(\frac{c}{a}\right)^{0.14} - 0.1066\left[1 + 1.5\left(\frac{c}{a}\right)\right] \times \left(\frac{a}{c}\right)^{1/2}\left(\frac{a}{t}\right) \quad (12)$$

for $1 \leqslant (a/c) \leqslant 2$, $(a/t) \leqslant 0.6$ and $(c/b) \leqslant 0.2$, where b is the half-width of the cracked specimen.

If $(c/b) > 0.2$, the correction functions Y_A, Y_B have to be multiplied by a finite-width correction f_w given [9] by

$$f_w = \left\{\sec\left[\frac{\pi c}{2b}\left(\frac{a}{t}\right)^{1/2}\right]\right\}^{1/2} \quad (13)$$

4.2.2. Averaged stress intensity factors

For brittle materials the question arises whether crack growth and also unstable fracture are governed by the local values of the stress intensity factor at the considered point of the crack front. It seems to be necessary to use an average K value taking into account neighboured K values near this location. Cruse and Besuner [10] proposed averaged stress intensity factors in fatigue crack growth evaluation, calculated by

$$\overline{Y_A^2} = \frac{4}{\pi}\int Y^2(\phi)\sin^2(\phi)\,d\phi \quad (14)$$

and

$$\overline{Y_B^2} = \frac{4}{\pi}\int Y^2(\phi)\cos^2(\phi)\,d\phi \quad (15)$$

for the points A and B at the crack contour.

Since the function $Y(\phi)$ is given by published formulae [9], the numerical evaluation of Equations 14 and 15 can be easily performed for $(a/c) \leqslant 1$. In case of $1 < (a/c) \leqslant 2$ the results tabulated [9] can roughly be expressed by

$$\bar{Y}_A \simeq 1.2\left(\frac{c}{a}\right)^{0.55} - \left[0.82 + 0.53\left(\frac{c}{a}\right)\right]\left(\frac{a}{t}\right) \quad (16)$$

$$\bar{Y}_B \simeq 1.47 - 0.23\left(\frac{a}{c}\right) - \left[0.425 + 0.35\left(\frac{c}{a}\right)\right]\left(\frac{a}{t}\right) \quad (17)$$

for $(a/t) < 0.5$ and $(c/b) < 0.2$.

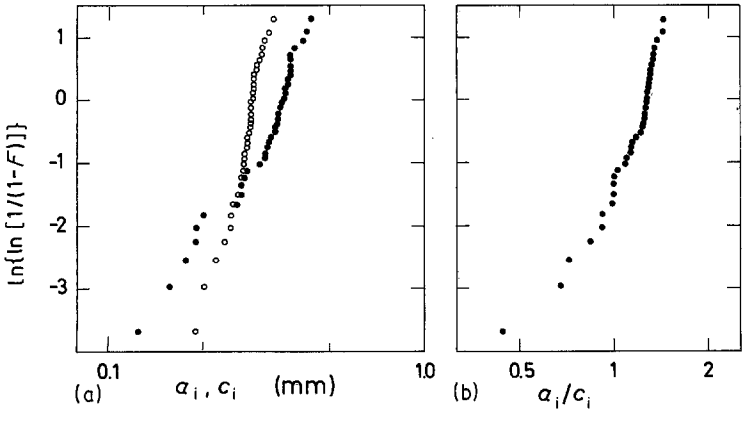

Figure 3 Cumulative distribution function F of (a) the initial crack data for (●) and (○) a_i, c_i, and (b) the initial aspect ratio a_i/c_i.

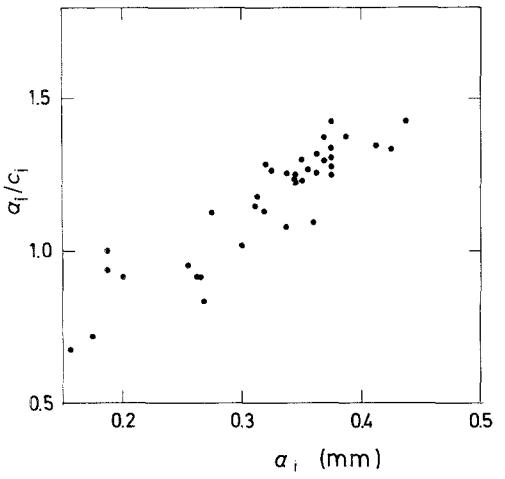

Figure 4 Relation between the initial aspect ratio and the initial crack depth.

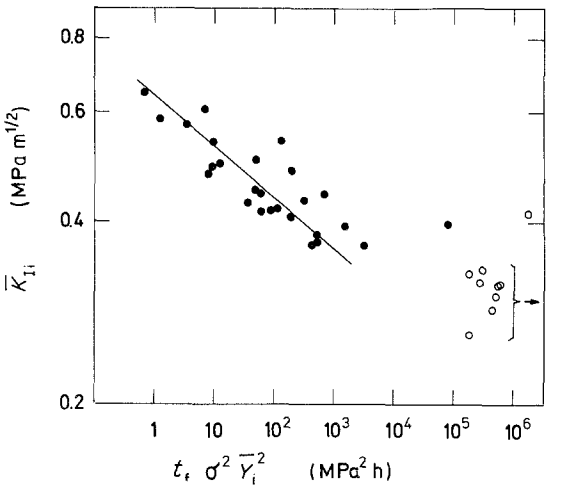

Figure 6 $\bar{K}_{Ii}$ against $t_f\sigma^2\overline{Y_i^2}$ for evaluating Equation 8.

Fig. 5 shows the geometric functions $\bar{Y}_A$ and $\bar{Y}_B$ in the depth range of $0 \leqslant (a/t) \leqslant 0.1$. For the range of measured aspect ratios one can approximately conclude

$$\bar{Y}_A,\ \bar{Y}_B \simeq \frac{2}{\pi^{1/2}} \pm 0.2$$

4.3. Evaluation

For evaluating Equation 8, first $\overline{K_{Ii}}$ was plotted against $t_f\sigma^2\overline{Y_i^2}$ (Fig. 6). In this representation the scatter of data points is evidently reduced compared with Fig. 2. For $\overline{K_{Ii}} > 0.3\,\mathrm{MPa\,m^{1/2}}$ the curve is approximately a straight line. The slope is found to be

$$\frac{\mathrm{d}[\log(\overline{K_{Ii}})]}{\mathrm{d}[\log(\sigma^2 t_f \overline{Y_i^2})]} = -0.0837$$

in this range.

This indicates that the crack growth law can be expressed by the power law of Equation 6, for not too low crack growth rates. In this case it results by use of the approximation of Equation 7 that

$$\frac{\mathrm{d}[\log(\bar{K}_{Ii})]}{\mathrm{d}[\log(\sigma^2 t_f \overline{Y_i^2})]} = \frac{-1}{n-2}$$

and hence $n = 13.9$ in accordance with literature data [1, 2].

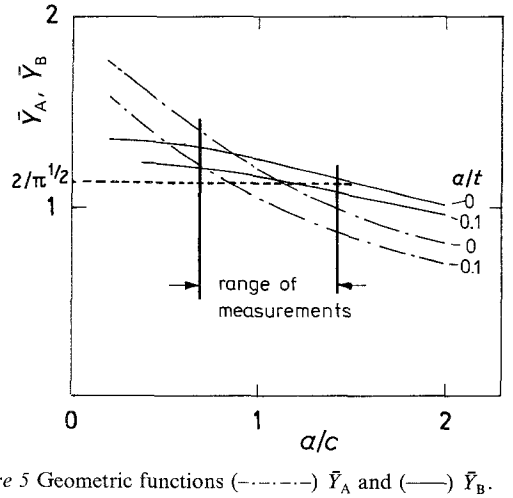

Figure 5 Geometric functions (–·–·–·–) $\bar{Y}_A$ and (——) $\bar{Y}_B$.

After determination of $\bar{Y}_i$ using Equation 11 and calculation of the initial stress intensity factors by applying Equation 1, the v–K_I curve represented in Fig. 7 was evaluated using Equation 5 and the slope in Fig. 6 of -0.0837. For values $\bar{K}_I \geqslant 0.35\,\mathrm{MPa\,m^{1/2}}$ a power law with $n = 14$ can be obtained. For $\bar{K}_I < 0.35\,\mathrm{MPa\,m^{1/2}}$ no crack growth is detectable and a threshold stress intensity factor $\bar{K}_{Ith}$ is found to be

$$\bar{K}_{Ith} \simeq 0.35\,\mathrm{MPa\,m^{1/2}}$$

The crack growth law can be written

$$v = 0.010\,\mathrm{MPa^{-14}\,m^{-6}\,sec^{-1}}\,\bar{K}_I^{14} \quad \text{for } \bar{K}_I \geqslant 0.35\,\mathrm{MPa\,m^{1/2}}$$

$$v = 0 \quad \text{for } \bar{K}_I < 0.35\,\mathrm{MPa\,m^{1/2}} \tag{18}$$

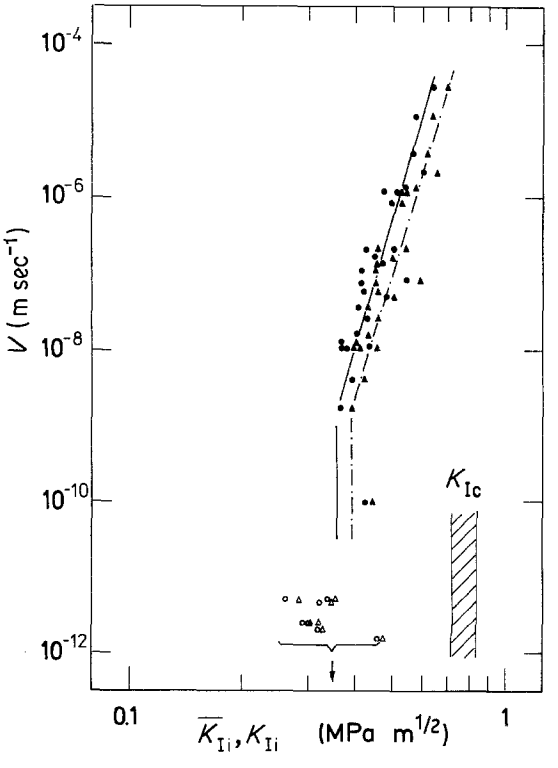

Figure 7 Crack growth law resulting from Equation 8. (●, ——) $\bar{K}_I$; (▲, –·–·–·–) K_I.

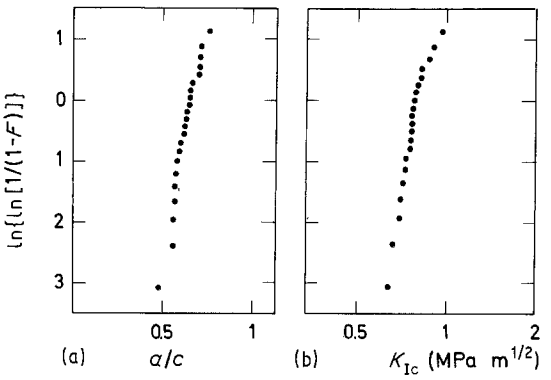

Figure 8 Weibull representation of (a) the aspect ratio at failure and (b) the fracture toughness K_{Ic}.

In addition, the same procedure was performed once more but now using local stress intensity factors. The results are also plotted in Fig. 7. The crack growth law obtained is given by

$$v = 0.0016\,\mathrm{MPa}^{-14}\,\mathrm{m}^{-6}\,\mathrm{sec}^{-1}\,\bar{K}_I^{14} \quad \text{for } K_I \geqslant 0.38\,\mathrm{MPa\,m}^{1/2}$$

$$v = 0 \quad \text{for } K_I < 0.38\,\mathrm{MPa\,m}^{1/2} \qquad (19)$$

As the crack dimensions at failure had been measured too, the median value of the fracture toughness was determined as $\langle K_{Ic} \rangle = 0.78\,\mathrm{MPa\,m}^{1/2}$ with a Weibull modulus of $m(K_{Ic}) = 10.0$ (Fig. 8). In contrast to the initial cracks the aspect ratio at failure was found to be significantly smaller, $\langle a/c \rangle_f = 0.61$, and a distinctly higher Weibull modulus resulted, namely $m(a/c)_f = 11.7$ (Fig. 8).

To understand this behaviour, the time-dependent crack development was calculated step by step. Starting with the initial crack quantities a_i and c_i the accompanying correction functions $\bar{Y}_A$ and $\bar{Y}_B$ were computed. For $(a/c) \leqslant 1$ the well-known formulae [9] were applied and in the case of $(a/c) > 1$ Equations 13, 16 and 17 were used.

The operative stress intensity factors $\overline{K_{IA}}$ and $\overline{K_{IB}}$ result from Equation 1. In the time step dt the crack size increments were computed as

$$da = v(\overline{K_{IA}})\,dt$$

$$dc = v(\overline{K_{IB}})\,dt$$

where the crack growth law $v(K_I)$ is given by Equation 18. The crack increments were added to the old values

$$a \rightarrow a + da$$

$$c \rightarrow c + dc$$

and the shape of the crack regarded as remaining semi-elliptical. For the following time steps the whole procedure had to be repeated until the maximum $\bar{K}_I$ factor reached the fracture toughness K_{Ic}.

Fig. 9 shows the development of the crack shape for two bending stresses. It can be seen that the initial relatively high scatter of a_i/c_i is already strongly reduced after a small amount of crack extension in depth. The crack shape at failure for a given stress is independent of the initial value after some crack extension, influenced only by the different stresses

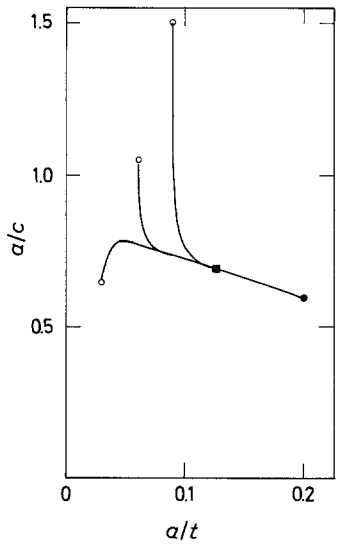

Figure 9 Development of the aspect ratio during crack extension for two bending stresses. (■) Failure for $\sigma = 25\,\mathrm{MPa}$; (●) failure for $\sigma = 20\,\mathrm{MPa}$; (○) starting point.

applied. From this point of view the measured crack data at failure can be understood completely.

5. Summary

A method is presented to determine subcritical crack growth rates from lifetime measurements on Knoop-damaged bending bars and especially outlined for the case of directly measurable crack dimensions.

The procedure is a modification of a technique proposed earlier [8] where the variation of the stress intensity factors applied was due to the scatter of natural crack sizes. Here the variation is adjusted by the application of different stresses.

As a model material glass in water was investigated, and by crack size measurements after failure its fracture toughness was found to be $K_{Ic} = 0.78\,\mathrm{MPa\,m}^{1/2}$. The resulting v–K_I curve can be described by a power law with an exponent $n = 14$ for $K_I > 0.35\,\mathrm{MPa\,m}^{1/2}$ and by a threshold value of about $K_{Ith} = 0.35\,\mathrm{MPa\,m}^{1/2}$ below which no subcritical crack growth could be detected. Thus the existence of a threshold in glass at first observed by Wiederhorn and Bolz [1] and Evans [2] could be confirmed. The measured threshold value is in good agreement with results reported by Simmons and Freiman [11] for borosilicate glass.

The crack data at failure can be obtained from the initial data by stepwise calculation of the crack development.

Acknowledgement

The authors wish to express their gratitude to the Deutsche Forschungsgemeinschaft for financial assistance.

References

1. S. M. WIEDERHORN and L. H. BOLZ, *J. Amer. Ceram. Soc.* **53** (1970) 543.
2. A. G. EVANS, *J. Mater. Sci.* **7** (1972) 1137.
3. P. FOURNIER and F. NAUDIN, *Rev. Phys. Appl.* **12** (1977) 797.
4. E. R. FULLER and R. M. THOMSON, "Fracture Mechanics of Ceramics", Vol. 4 edited by R. G. Bradt, A. G. Evans, D. P. H. Hasselman and F. F. Lange (Plenum, New York, 1978) pp. 507–548.

5. B. R. LAWN, *J. Mater. Sci.* **10** (1975) 469.
6. T. FETT and D. MUNZ, "Zur Deutung des unterkritischen Rißwachstums keramischer Werkstoffe", DFVLR-FB 82-07 (Deutsche Forschungs- und Versuchsanstalt für Luft- and Raumfahrt, Cologne, 1982).
7. T. FETT, "Prediction of lifetime for ceramic materials in the elastic and viscoelastic region by fracture mechanical methods," ESA-TT-825 (European Space Agency, Cologne, 1984).
8. T. FETT and D. MUNZ, *Commun. Amer. Ceram. Soc.* **68** (1985) C213.
9. J. C. NEWMAN and I. S. RAJU, "Analyses of surface cracks in finite plates under tension or bending loads," NASA Technical Paper 1578 (NASA, Hampton, 1979).
10. T. A. CRUSE and P. M. BESUNER, *J. Aircraft* **12** (1975) 369.
11. C. J. SIMMONS and S. W. FREIMAN, *J. Amer. Ceram. Soc.* **64** (1981) 683.

Received 9 September 1986
and accepted 18 June 1987